ELSEVIER

Journal of Food Engineering **29** (1996) 399–414

0260-8774/96/$15.00 + 0.00

PII: S0260-8774(96)00008-8

Analysis of Heat, Mass and Pressure Transfer in Starch Based Food Systems

Yun Wu[a] & Joseph Irudayaraj[b]*

[a]Agricultural and Bioresource Engineering, University of Saskatchewan, Saskatoon, Saskatchewan S7N 0W0, Canada
[b]Biological and Irrigation Engineering, Utah State University, Logan, Utah 84322-4105, USA

(Received 26 September 1994; accepted 5 February 1996)

ABSTRACT

A set of coupled heat, mass and pressure transfer equations proposed by Luikov (1975, Heat and mass transfer in capillary-porous bodies, Pergamon, UK) was employed to model the heat, mass and pressure transfer phenomenon in a composite food system during drying. A two-dimensional finite element model was developed to solve the coupled equations with non-linear material properties. The finite element results were validated by comparing with exact solutions. The validated finite element model was then used to predict the temperature and moisture history in hydrated composite starch systems. Comparison of predictions from the coupled and uncoupled heat and mass transfer models, which assumed that pressure is a constant, with the experimental data showed a marked difference. Simulation results indicated that predictions from the heat, mass and pressure transfer model agreed well with the available experimental data. Copyright © 1996 Elsevier Science Limited

NOTATION

a_m	Mass diffusion coefficient (m^2/s)
c_m	Specific moisture capacity ($kg_{moisture}/kg_{drybody}$)
c_p	Air capacity ($kgm^2/kg.N$)
c_q	Heat capacity (J/kg^0K)
j_m	Specific mass flux ($kg_{moisture}/m^2s$)
j_q	Specific heat flux (W/m^2)
k_m	Coefficient of moisture conductivity (kg/m.h.°M)

*Author to whom correspondence should be addressed.

k_p Moisture filtration coefficient (kg.m/s.N)
k_q Thermal conductivity (W/m°K)
m Moisture content (% kg water/kg solid)
M Moisture potential (°M)
n Number of nodes in element
P Pressure (kN/m^2)
t Time (s)
T Temperature (°C)

Greek letters
α_m Convective mass transfer coefficient (kg moisture/m^{2}s)
α_q Convective heat transfer coefficient (W/m^2°K)
δ Thermo-gradient coefficient (1/°K)
λ Latent heat (J/kg)
Ω Domain of interest (m^3)
ρ_o Dry body density (kg/m^3)
Γ Surface boundary (m^2)
ϕ Vector of unknowns [T M P]^T
ε Ratio of vapor diffusion coefficient to the coefficient of total moisture diffusion

Subscripts
a Ambient
m Mass
o Prescribed
q Heat

INTRODUCTION

The analysis of heat and mass transfer in a food system is very important because food properties change with temperature and moisture movement during drying. Various models have been proposed to predict the temperature and moisture movement in food grains (Irudayaraj *et al.*, 1992). Kinetic models have been used in water excess food system (Wirakartakusumah, 1981). Keey (1972) pointed out that such kinetic models may be unduly restrictive because of the complex nature of starch based systems. Whitaker *et al.* (1969) recognized that moisture diffusion equation is not adequate for describing the moisture movement process. The transfer of moisture and heat must be considered simultaneously. The interrelation between heat and mass transfer was described by Luikov's coupled system of partial differential equation (Luikov, 1975). Luikov conducted a large number of investigations to validate the theory and determine experimentally the value of the parameters for a number of materials.

Most of previous studies on capillary materials were based on Luikov's two term (temperature term and moisture term) model which assumed that pressure was constant throughout the domain (Irudayaraj *et al.*, 1992). Recent studies by Lewis & Ferguson (1990) and Irudayaraj & Wu (1994), based on Luikov's three term (temperature, moisture and pressure) model revealed that, during an intense drying process, a pressure gradient develops inside the capillary porous body, which causes

moisture transfer by filtration, in addition to moisture transfer by diffusion. Previous studies focussed either on a one-dimensional system or the model predictions were not verified with experimental results. Applicability of the coupled model to a composite starch-based system has not been done.

Sakai & Hayakawa (1992) presented a mathematical model to predict the heat and moisture transfer in a composite food system. In their study, the temperature and moisture dependent transport properties were considered, and the moisture transfer potential was replaced by the chemical potential of water. However, in the experimental validation, the thermal dependency of mass transfer (Dufour effect) and mass dependency of heat transfer (Soret effect) were neglected. The present study will focus on applying Luikov's coupled three term (temperature, moisture and pressure term) model to study the transport process in a composite food system and to evaluate the effect of the inter-dependency of heat and mass transfer and the effect of pressure gradient on temperature and moisture movement.

The objectives of this study are to: (1) present a two-dimensional finite element formulation of a set of coupled heat, mass and pressure transfer equations; (2) validate the model by comparing the model predictions with exact solutions for a simplified system; (3) apply the validated finite element model to predict the temperature, moisture and pressure variation in a hydrated composite food system and compare with the available experimental data, and predictions from the uncoupled and coupled heat and mass transfer models.

THEORETICAL ANALYSIS

Governing equations

The coupled system of partial differential equations (Luikov, 1975) for temperature, moisture potential and pressure can be simplified (Lewis & Ferguson, 1990) and presented as:

$$C_q \frac{\partial T}{\partial t} = K_{11}\nabla^2 T + K_{12}\nabla^2 M + K_{13}\nabla^2 P \tag{1}$$

$$C_m \frac{\partial M}{\partial t} = K_{21}\nabla^2 T + K_{22}\nabla^2 M + K_{23}\nabla^2 P \tag{2}$$

$$C_p \frac{\partial P}{\partial t} = K_{31}\nabla^2 T + K_{32}\nabla^2 M + K_{33}\nabla^2 P \tag{3}$$

where moisture content was expressed by the moisture potential as, ($m = c_m M$). The coefficients C_q, C_m, C_p, K_{11}, K_{12}, K_{13}, K_{21}, K_{22}, K_{23}, K_{31}, K_{32} and K_{33} are functions of temperature and moisture transfer properties and are given by

$$C_q = \rho_0 c_q \delta / c_m;\ C_m = \varepsilon\lambda\rho_0 c_m;\ C_p = -\lambda\rho_0 c_p k_p / \mathrm{k_m}$$

$$K_{11} = (k_q + \varepsilon\lambda k_m)\delta/c_m;\ K_{12} = \varepsilon\lambda k_m \delta/c_m;\ K_{21} = \varepsilon\lambda k_m \delta/c_m$$

$$K_{22} = \varepsilon\lambda k_m;\ K_{13} = \varepsilon\lambda k_p \delta/c_m;\ K_{31} = \varepsilon\lambda k_p \delta/c_m$$

$$K_{33} = -\lambda(1-\varepsilon)k_p^2/k_m;\ K_{23} = \varepsilon\lambda k_p;\ K_{32} = \varepsilon\lambda k_p$$

The boundary conditions associated with this system of equation was written in a generalised form as

$$(k_g+\varepsilon\lambda\rho_o\delta a_m)\frac{\partial T}{\partial n}+J_q^* = 0 \tag{4}$$

$$a_m\frac{\partial M}{\partial n}+J_m^* = 0 \tag{5}$$

where

$$J_q^*=A_q(T-T_a)+A_\varepsilon(M-M_a)+J_q \tag{6}$$

$$J_m^* = A_\delta(T-T_a)+A_m(M-M_a)+J_m \tag{7}$$

and

$$A_q = \frac{(k_q+\varepsilon\lambda\rho_o\delta a_m)\alpha_q}{k_q}$$

$$A_\varepsilon = \frac{\lambda\rho_o\alpha_m}{k_q}(1-\varepsilon)(k_q+\varepsilon\lambda\rho_o\delta a_m)$$

$$A_\delta = -\frac{a_m\delta\alpha_q}{k_q}$$

$$A_m = \alpha_m - \frac{a_m\alpha_m\rho_0\lambda\rho}{k_q}(1-\varepsilon)$$

$$J_q = \frac{k_q+\varepsilon\lambda\rho_0\delta a_m}{k_q}$$

$$J_m = \frac{j_m}{\rho_0} - \frac{a_m\delta j_q}{k_q}$$

FINITE ELEMENT FORMULATION

The governing differential equations [eqn (1)eqn (2)eqn (3)] were transformed into element equations by using the Galerkin's weighted residual method. The dependent variables T, M and P were approximated in terms of the respective nodal values T_j, M_j and P_j by interpolating functions as:

$$T = \sum_{j=1}^{n} N_j(x,y)T_j(t) \tag{8}$$

$$M=\sum_{j=1}^{n} N_j(x,y)M_j(t) \tag{9}$$

$$P=\sum_{j=1}^{n} N_j(x,y)P_j(t) \tag{10}$$

where N_j is the weighting function and n is the number of nodes in the element. Using the Galerkin weighted residual method and setting the residual of the weighted errors to zero, eqns (1–3) can be written as

$$\int_{\Omega} N_i\left[\nabla\cdot(K_{11}\nabla\bar{T})+\nabla\cdot(K_{12}\nabla\bar{M})+\nabla\cdot(K_{13}\nabla\bar{P})-C_q\frac{\partial\bar{T}}{\partial t}\right]d\Omega=0 \tag{11}$$

$$\int_{\Omega} N_i\left[\nabla\cdot(K_{21}\nabla\bar{T})+\nabla\cdot(K_{22}\nabla\bar{M})+\nabla\cdot(K_{23}\nabla\bar{P})-C_m\frac{\partial\bar{M}}{\partial t}\right]d\Omega=0 \tag{12}$$

$$\int_{\Omega} N_i\left[\nabla\cdot(K_{31}\nabla\bar{T})+\nabla\cdot(K_{32}\nabla\bar{M})+\nabla\cdot(K_{33}\nabla\bar{P})-C_p\frac{\partial\bar{P}}{\partial t}\right]d\Omega=0 \tag{13}$$

Applying Green's theorem (integration by parts) and introducing the generalized boundary conditions (eqns (4–7)) and further simplifying, the above expressions can be written in a matrix form (Irudayaraj & Wu, 1994) as

$$[\mathbf{C}(\phi)]\{\dot{\phi}\}+[\mathbf{K}(\phi)]\{\phi\}+\{\mathbf{F}\}=\{0\} \tag{14}$$

where

$\{\phi\}^T = [T\ M\ P]$
$\mathbf{C}(\phi)$ = global capacitance matrix
$\mathbf{K}(\phi)$ = global conductance matrix
$\{\mathbf{F}\}$ = global force vector.

Equation (14) can be solved using Lees three level scheme (Comini *et al.*, 1976; Comini *et al.*, 1974; Irudayaraj *et al.*, 1990).

VALIDATION OF THE FINITE ELEMENT MODEL

The two dimensional finite element predictions were compared with the exact solutions for the values of coefficients in eqn (1–3) as given in Table 1. The exact solution for this system was given by:

$$T(x,y,t)=e^{x+y+t}+C_1 \tag{15}$$

TABLE 1
Coefficient Matrix

Coefficient	*Value*	*Coefficient*	*Value*	*Coefficient*	*Value*
C_q	5·25	C_m	10·5	C_p	21·0
K_{11}	2·0	K_{12}	1·0	K_{13}	0·5
K_{21}	2·0	K_{22}	1·0	K_{23}	0·5
K_{31}	2·0	K_{32}	1·0	K_{33}	0·5

$$M(x,y,t) = 0{\cdot}5^{*}e^{x+y+t}+C_2 \tag{16}$$

$$P(x,y,t) = 0{\cdot}25^{*}e^{x+y+t}+C_3 \tag{17}$$

The constants C_1, C_2, and C_3 can be determined using the initial conditions. The two dimensional finite element grid (0·14 × 0·15 m cross section) was discretized into 14 × 14 uniform nine-noded Lagrangian elements. Figure 1 is a comparison of finite element predictions (dimensionless) with the exact solution at the corresponding location (x = 0·06 m, y = 0·07 m). It can be seen that the temperature, moisture, and pressure predictions agree well with the exact solutions.

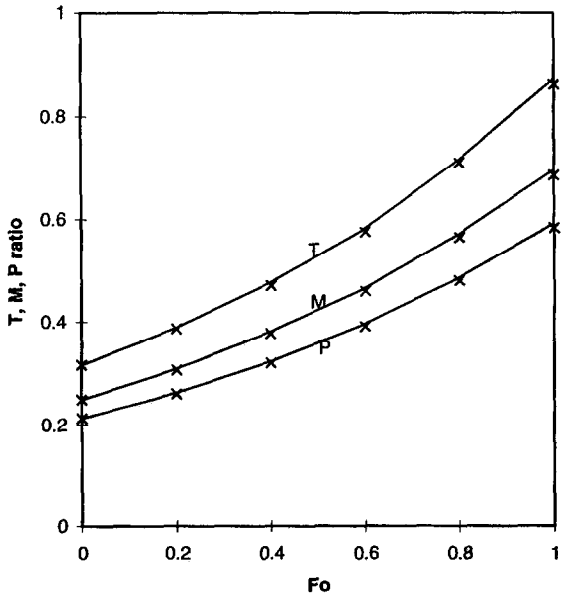

Fig. 1. Comparison of finite element predicted temperature, moisture and pressure ratio (solid line) with exact solution (symbols) at x = 0·06 m and y = 0·07 m).

Application

The finite element model was used to study the drying of hydrated starch samples. The composite system comprised of three cylindrical layers arranged in two different ways. In one arrangement (HSH), S sample was in the middle and H samples formed the outer layers. In another arrangement (SHS), H sample was in the middle and S samples formed the exterior. The S sample was formed by a hydrated mixture of sucrose (25%) and high amylose starch granules (75%) (S). The H sample was made from hydrates of high amylose starch granules (Sakai & Hayakawa, 1992). A two-dimensional finite element mesh in cylindrical coordinates was used to model a quarter of the composite cylindrical system (Fig. 2). The grid consisted of 42 nine-noded Lagrangian elements with a total of 255 nodes. The diameter of the sample was 28·6 mm. To obtain a solution to the set of heat, mass and pressure transfer equations, it is necessary to prescribe a set of boundary conditions. Boundary conditions considered are: (1) natural boundary conditions (convection or flux) and (2) essential boundary conditions (prescribed). Since axial symmetry was assumed, the fluxes across r and z axes (i.e., $z = 0$ and $r = 0$) are zero. There is no mass transfer across these edges and hence the boundaries appear as though they are insulated. Along the outer surface AB and BC convective conditions for heat and mass transfer and a prescribed boundary condition for pressure were assumed. Drying air temperature was 56°C. The initial temperature and moisture content of the sample were 25°C and 0·2 (g of H_2O/g of solid) respectively. The time step used in the simulation was 30 seconds for the first hour and 120 seconds for the rest of the drying period.

The material properties used in this simulation are given in Table 2. The value of moisture conductivity k_m and special moisture capacity c_m were obtained from Hallstrom *et al.* (1988). The value of thermogradient coefficient δ was obtained from

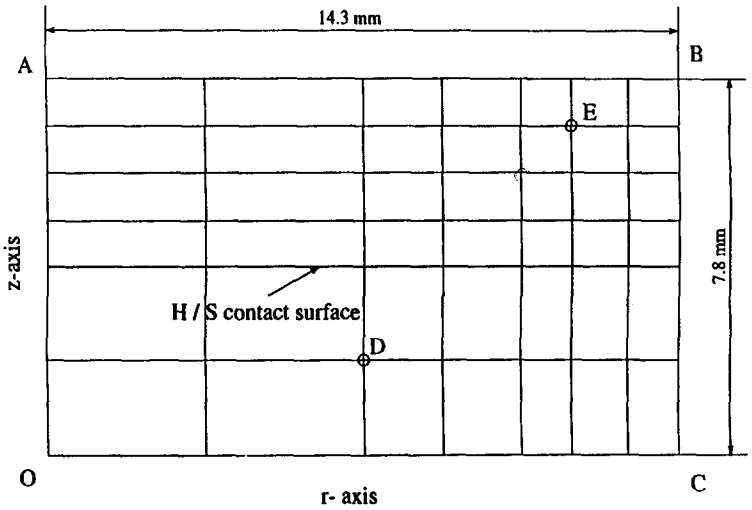

Fig. 2. Two-dimensional finite element mesh of the composite hydrated starch system in cylindrical coordinates.

TABLE 2
Material Properties

Material property	*Units*	*Hydrated starch*
ρ_o	kg/m^3	603 for H sample, 741 for S sample
k_q	J/m.K.s	0·3487+0·001162T+0·05811(M/(1+M))
c_q	J/kg.K	1895−12·09T+1733(M/(1+M))
k_p	kg.m/h.N	$0{\cdot}77 \times 10^{-7}$
c_p	m^2/N	0·08
ε		0·3
λ	J/kg	$2{\cdot}3 \times 10^6$
δ	1/K	0·015
c_m	kg/kg.°M	0·0017
h_m	m/h$_r$	200
h_q	W/m^{2}K	17·4

Irudayaraj (1992) for similar drying conditions. The moisture filtration coefficient k_p and vapour diffusion ratio ε used in this study were similar to the values used for a gel system (Lewis & Ferguson, 1990). Values of other properties were obtained from Sakai & Hayakawa (1992).

The following illustrations will compare predictions from Luikov's heat, mass and pressure transfer model (model 1) with the available experimental data (Sakai & Hayakawa, 1992). A second model (model 2) which assumes an independent heat and mass transfer state and constant pressure will also be used. This will give an indication of the effect of pressure and the inter-dependency of heat and mass transfer. The effect of pressure on heat and mass transfer will be demonstrated by comparing the coupled heat, mass, and pressure transfer model (model 1) and the coupled heat and mass transfer model (model 3). Model 2 and model 3 are simplified versions of model 1, and can be obtained from eqns (1–3) by setting the necessary coefficients to zero.

Figures 3 and 4 show the temperature variation at the center of HSH and SHS sample respectively. Results indicate that predictions from model 1 were closer to experimental data than that from model 2. The center temperature increased approximately linearly with drying time during the first half hour of drying and gradually reached a steady state after three hours. Model 2 is an uncoupled model in which moisture has no effect on the temperature. Model 1 accounts for internal evaporation, hence moisture is present in the liquid and vapor phases. The regions in which moisture is present in the vapor phase is at a higher temperature and this resulted in a higher temperature prediction from model 1.

Figures 5 and 6 compare the predicted average moisture concentration from model 1 and model 2 with experimental data, in the H and S layer of the SHS sample respectively. It can be clearly seen that model 1, which considers the coupled effect of heat and mass transfer and the effect of pressure gradient on temperature and moisture movement, fitted the experimental data better than model 2. Model 2 overpredicted by a maximum of 82% while model 1 overpredicted by a maximum of 12·5% (Fig. 5). After four hours of drying, the predicted results from model 1 and

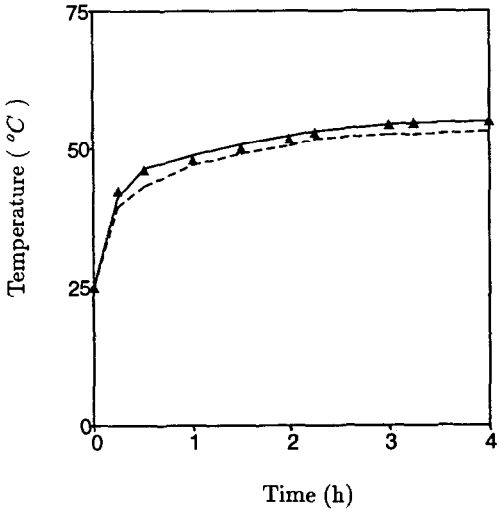

Fig. 3. Comparison of predicted central (Point O) temperature histories of HSH sample by model 1 (solid line) and model 2 (dashed line) with measured values (symbols), Sakai & Hayakawa (1992).

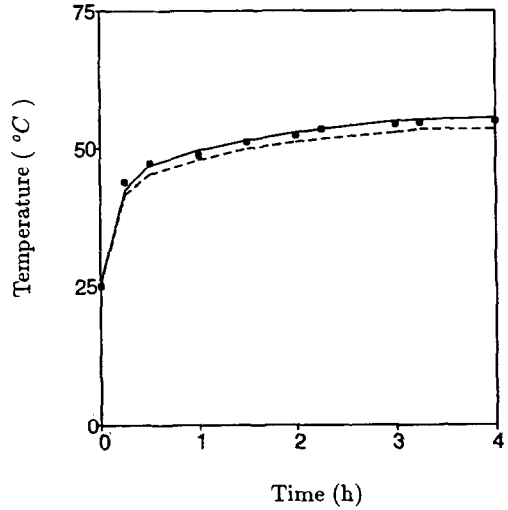

Fig. 4. Comparison of predicted central (Point O) temperature histories of SHS sample by model 1 (solid line) and model 2 (dashed line) with measured values (symbols), Sakai & Hayakawa (1992).

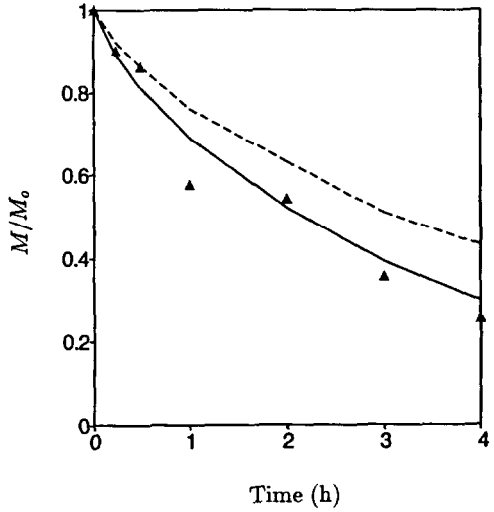

Fig. 5. Comparison of predicted average moisture histories of H layer of the SHS sample by model 1 (solid line) and model 2 (dashed line) with measured values (symbols), Sakai & Hayakawa (1992).

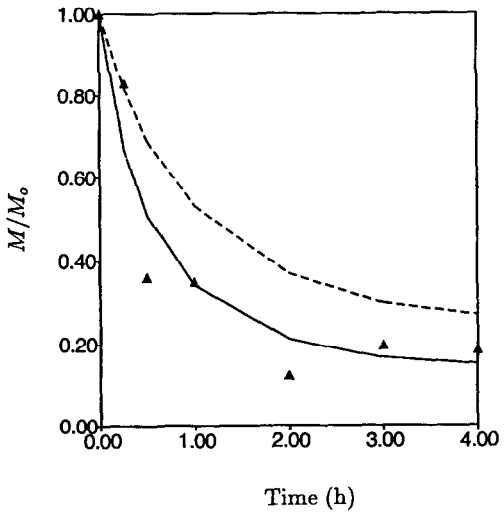

Fig. 6. Comparison of predicted average moisture histories of S layer of the SHS sample by model 1 (solid line) and model 2 (dashed line) with measured values (symbols), Sakai & Hayakawa (1992).

model 2 were 0·315 and 0·445 respectively while the measured moisture value was 0·28. Comparison of model predictions in the S layer (Fig. 6) indicated that model 1 and model 2 deviated by a maximum of 0·1 and 0·25 from the experimental data after two hours of drying.

Figures 7 and 8 present the predicted average moisture concentration in H and S layer of the HSH sample with experimental data. The maximum deviation of prediction (after two hours of drying) from model 2 was 0·17 while that from model 1 had a fair agreement with the experimental results (maximum deviation was 0·06). This could be attributed to the fact that the effect of pressure gradient and the inter-dependency of heat and mass transfer was not considered in model 2. Figure 8 shows a similar trend in model predictions. The deviation of moisture content predictions from the measured values could be due to the change of water activity in S layer because it was made from a mixture of 25% sucrose and 75% high amylose starch. The sudden change in temperature (Figs 3 and 4) and moisture content (Figs 5–8) during the initial stages (1 h) of drying indicates an increased temperature and moisture gradient, which contributes to a faster drying rate. Once the temperature gradients are established their dependence on moisture transfer decreases, hence during the later stages drying occurs mostly due to the presence of moisture gradient. As the moisture gradient decreases drying rate decreases and the moisture content in the sample approaches an equilibrium state.

Figures 9 and 10 show the respective pressure profile in the HSH and SHS sample at location D ($r = 7{\cdot}15$ mm, $z = 1{\cdot}95$ mm), and E ($r = 11{\cdot}92$ mm, $z = 6{\cdot}925$ mm) as pointed out in Fig. 2. The pressure gradient gives rise to additional moisture transfer due to filtration effect. It can be seen that pressure varies more rapidly at the surface that the center. Increased variation at the surface, gives rise to larger gradients in regions closer to the surface than the centre. Hence, the

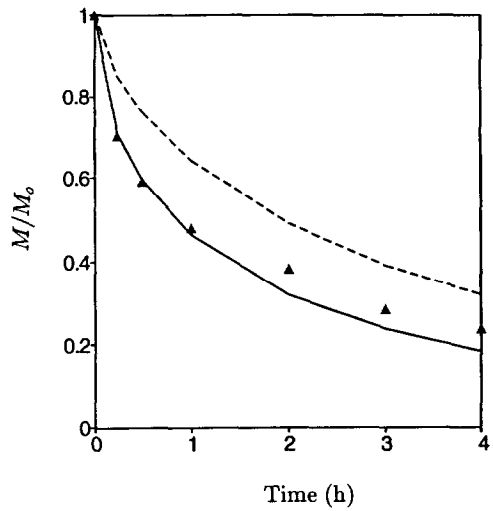

Fig. 7. Comparison of predicted average moisture histories of H layer of the HSH sample by model 1 (solid line) and model 2 (dashed line) with measured values (symbols), Sakai & Hayakawa (1992).

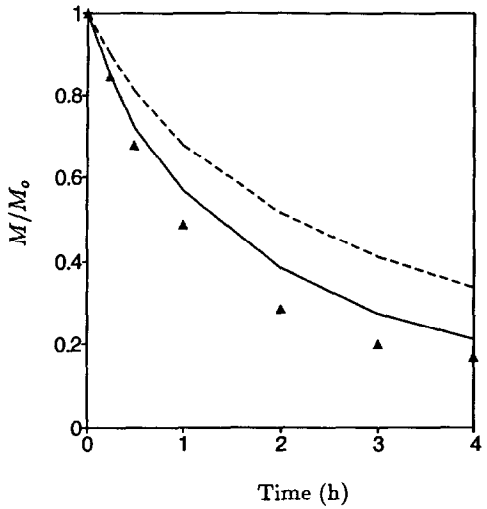

Fig. 8. Comparison of predicted average moisture histories of S layer of the HSH sample by model 1 (solid line) and model 2 (dashed line) with measured values (symbols), Sakai & Hayakawa (1992).

contribution of pressure gradient to moisture transfer is larger at the surface, while this effect may be negligible in the inner regions.

Figures 11 and 12 present the effect of pressure on the predicted mass average moisture ratio of the SHS and HSH samples using model 1 (coupled heat, mass and

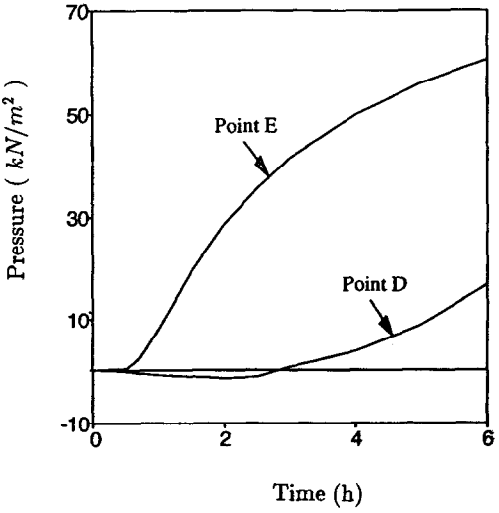

Fig. 9. Pressure variation at point D ($r = 7{\cdot}15$ mm, $z = 1{\cdot}95$ mm) and point E ($r = 11{\cdot}92$ mm, $z = 6{\cdot}925$ mm) in HSH sample.

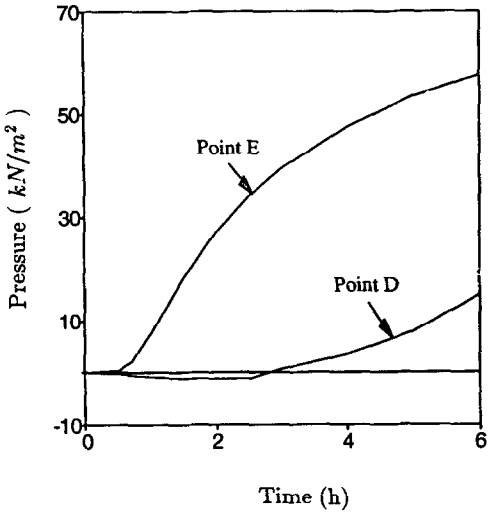

Fig. 10. Pressure variation at point D ($r = 7{\cdot}15$ mm, $z = 1{\cdot}95$ mm)

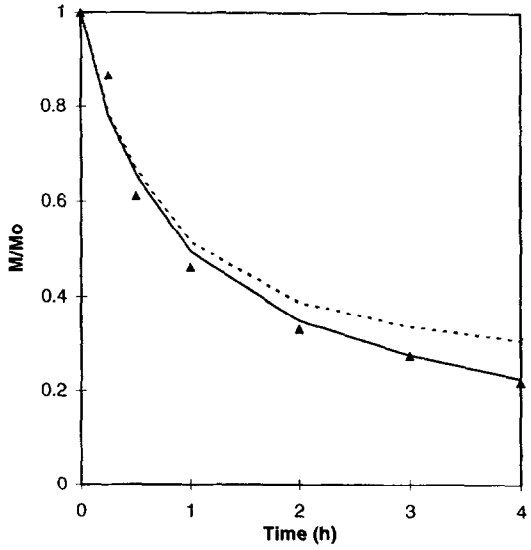

Fig. 11. Comparison of predicted mass average moisture histories of the SHS sample by model 1 (solid line) and model 3 (dashed line) with measured values (symbols), Sakai & Hayakawa (1992).

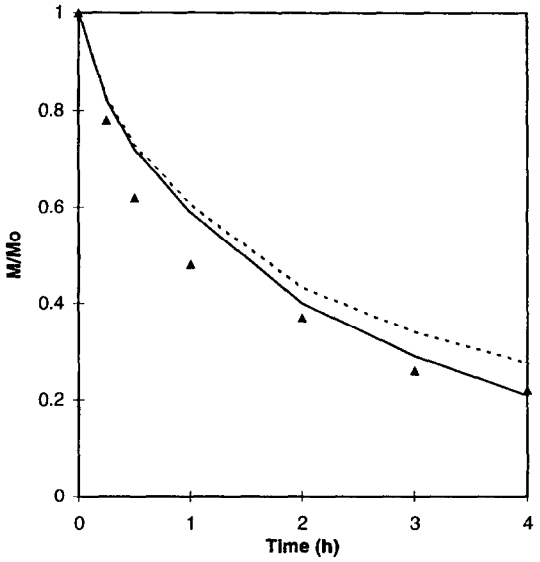

Fig. 12. Comparison of predicted mass average moisture histories of the HSH sample by model 1 (solid line) and model 3 (dashed line) with measured values (symbols), Sakai & Hayakawa (1992).

pressure transfer) and model 3 (coupled heat and mass transfer model with constant pressure) for a drying temperature of 56°C. The deviation of moisture prediction by model 3, from experimental data (Sakai & Hayakawa, 1992) was significantly greater than that from model 1. Model 1 considers the additional moisture movement caused by pressure gradient and model 3 does not account for this additional moisture transfer. The excess moisture movement that can be attributed to the effect of the pressure was 2·5% and 2·2% for the SHS (Fig. 11) and HSH (Fig. 12) sample. Under such circumstances, omission of the pressure term will result in an over prediction of moisture content. There was no noticeable difference in temperature prediction between the two models. Hence the comparison for temperature prediction was not presented.

Figure 13 shows the effect of drying temperature on the average moisture content of HSH sample. Model 1 was used in this simulation because of its better fit (Figs 3–8) with the experimental data. to the initial moisture content of HSH sample was 0·185 for the drying temperature of 70°C, while the ratio was 0·22 and 0·325 for drying temperatures of 56°C and 40°C respectively. The predicted results for SHS sample were similar to those for HSH sample hence were not reported.

CONCLUSIONS

The temperature, moisture and pressure distribution in a composite food system during drying was described by a set of coupled non-linear heat, mass and pressure transfer equations. The finite element method was used to solve the system of

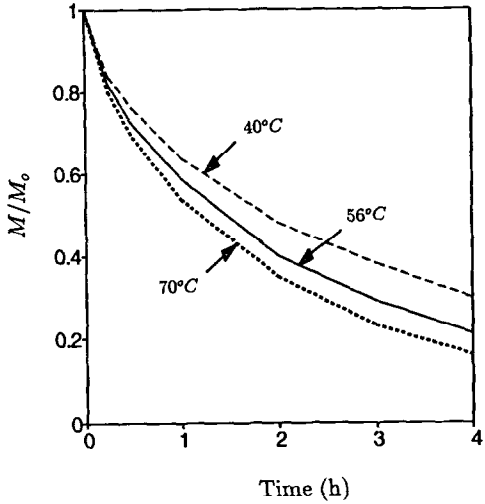

Fig. 13. Effect of drying temperature on the average moisture variation of HSH sample.

equations. A two dimensional cylindrical coordinate system was used. The finite element predictions were in excellent agreement with the exact solutions.

The simulation study in the composite starch food system showed that the finite element predictions from Luikov's heat, mass and pressure transfer model agreed well with the experimental data. However, prediction from the uncoupled heat and mass transfer model showed a considerable difference with the experimental results. This was due to the fact that the inter-dependency of heat transfer and mass transfer and the effect of pressure gradient on moisture movement were not taken into account in the uncoupled heat and mass transfer model. Comparison of pressure dependent (model 1) and pressure independent (model 3) coupled models indicated that pressure gradient causes additional moisture transfer. Hence, the application of Luikov's coupled transfer equations to complex food systems, which neglected the dependency of heat and mass transfer or assumed a constant pressure, should be used with caution.

REFERENCES

Comini, G. & Lewis, R. W. (1976). A numerical solution of two-dimensional problems involving heat and mass transfer. *Int. J. Heat Mass Transfer*, **19**, 1387–9.2

Comini, G., Guidice, D. S., Lewis, R. W. & Zienkiewicz, O. C. (1974). Finite element solution of nonlinear heat conduction problems with special reference to phase change. *Int. J. Num. Meth. in Eng.*, **8**, 613–24.

Hallstrom, B., Skjoldebrand, C. & Tragardh, C. (1988). *Heat transfer and food products*, 19-22, Elsevier Applied Science, London and New York.

Irudayaraj, J., Haghighi, K. & Stroshine, R. L. (1990). Nonlinear finite element analysis of coupled heat and mass transfer problems with an application to timber drying. *Drying Technology*, **8** (4), 731–49.

Irudayaraj, J., Haghighi, K. & Stroshine, R. L. (1992). Finite element analysis of drying with application to cereal grains. *J. Agric. Engng. Res.*, **53** (4), 209–29.

Irudayaraj, J. & Wu, Y. (1994). Finite element solution of coupled heat, mass and pressure transfer in porous biomaterials. *Int. J. of Numerical Heat Transfer*, **26(2)**

Keey, R. B. (1972). *Drying: Principles and practice, NY.* Pergamon Press, New York.

Lewis, R. W. & Ferguson, W. J. (1990). The effect of temperature and total gas pressure on the moisture content in a capillary porous body. *Int. J. For Numerical Methods In Engineering*, **29**, 357–69.

Luikov, A. V. (1975). *Heat and Mass Transfer in Capillary-Porous Bodies*, Pergamon Press, Oxford, UK.

Sakai, N. & Hayakawa, K. I. (1992). Two dimensional simultaneous heat and moisture transfer in composite food. *J. Food Science*, **57** (2), 475–80.

Whitaker, T. B., Barre, H. J. & Hamdy, M. Y. (1969). Theoretical and experimental studies of diffusion in spherical bodies with a variable diffusion coefficient. *Transactions of The ASAE*, **12** (5), 668–72.

Wirakartakusumah, M. A. (1981). Kinetics of starch gelatinization and water absorption in rice. Ph.D. Dissertation. Dep. Food Sci. University of Wisconsin, Madison.